# Compact wavelength demultiplexing using focusing negative index photonic crystal superprisms

**Babak Momeni, Jiandong Huang, Mohammad Soltani, Murtaza Askari, Saeed Mohammadi, Mohammad Rakhshandehroo and Ali Adibi**

*School of Electrical and Computer Engineering, Georgia Institute of Technology, Atlanta, GA 30332 USA*
momeni@ece.gatech.edu, jdhuang@ece.gatech.edu, soltani@ece.gatech.edu, murtaza@ece.gatech.edu, saeedm@ece.gatech.edu, adibi@ece.gatech.edu

**Abstract:** Here, we demonstrate a compact photonic crystal wavelength demultiplexing device based on a diffraction compensation scheme with two orders of magnitude performance improvement over the conventional superprism structures reported to date. We show that the main problems of the conventional superprism-based wavelength demultiplexing devices can be overcome by combining the superprism effect with two other main properties of photonic crystals, i.e., negative diffraction and negative refraction. Here, a 4-channel optical demultiplexer with a channel spacing of 8 nm and cross-talk level of better than -6.5 dB is experimentally demonstrated using a 4500 $\mu m^2$ photonic crystal region.

©2006 Optical Society of America

**OCIS codes:** (999.9999) Photonic crystals; (999.9999) Superprism; (130.3120) Integrated optics devices

## References and links

1. E. Yablonovitch, "Inhibited spontaneous emission in solid-state physics and electronics," Phys. Rev. Lett. **58**, 2059-2062 (1987).
2. S. John, "Strong localization of photons in certain disordered dielectric superlattices," Phys. Rev. Lett. **58**, 2486-2489 (1987).
3. S. G. Johnson and J. D. Joannopoulos, "Designing synthetic optical media: photonic crystals," Acta Materialia **51**, 5823-5835 (2003).
4. H. Kosaka, T. Kawashima, A. Tomita, M. Notomi, T. Tamamura, T. Sato, and S. Kawakami "Superprism phenomena in photonic crystals: toward microscale lightwave circuits," J. Lightwave Technol. **17**, 2032-2038 (1999).
5. H. Kosaka, T. Kawashima, A. Tomita, T. Sato, and S. Kawakami, "Photonic crystals for micro lightwave circuits using wavelength-dependent angular beam steering," Appl. Phys. Lett. **74**, 1370-1372 (1999).
6. M. Notomi, "Theory of light propagation in strongly modulated photonic crystals: Refractionlike behavior in the vicinity of the photonic band gap," Phys. Rev. B **62**, 10696-10705 (2000).
7. A. Lupu, E. Cassan, S. Laval, L. El Melhaoui, P. Lyan, and J. M. Fedeli, "Experimental evidence for superprism phenomena in SOI photonic crystals," Optics Express **12**, 5690-5696 (2004).
8. L. Wu, M. Mazilu, and T. F. Krauss, "Beam steering in planar-photonic crystals: from superprism to supercollimator," J. Lightwave Technol. **21**, 561-566 (2003).
9. T. Baba, and T. Matsumoto, "Resolution of photonic crystal superprism," Appl. Phys. Lett. **81**, 2325-2327 (2002).
10. B. Momeni and A. Adibi, "Optimization of photonic crystal demultiplexers based on the superprism effect," Appl. Phys. B **77**, 555-560 (2003).
11. C. Luo, M. Soljacic, and J. D. Joannopoulos, "Superprism effect based on phase velocities," Optics Lett. **29**, 745-747 (2004).
12. T. Matsumoto and T. Baba, "Photonic crystal *k*-vector superprism," J. Lightwave Technol. **22**, 917-922 (2004).
13. A. Bakhtazad, and A. G. Kirk, "1-D slab photonic crystal k-vector superprism demultiplexer analysis, and design," Optics Express **13**, 5472-5482 (2005).
14. B. Momeni and A. Adibi, "Preconditioned superprism-based photonic crystal demultiplexers: Analysis and design," (submitted to Applied Optics).

#67663 - $15.00 USD Received 3 February 2006; revised 9 March 2006; accepted 14 March 2006
(C) 2006 OSA

15. J. Witzens, T. Baehr-Jones, and A. Scherer, "Hybrid superprism with low insertion losses and suppressed cross-talk," Phys. Rev. E **71**, 026604-1-9 (2005).
16. T. Matsumoto, S. Fujita, and T. Baba, "Wavelength demultiplexer consisting of photonic crystal superprism and superlens," Optics Express **13**, 10768-10776 (2005).
17. A. Berrier, M. Mulot, M. Swillo, M. Qiu, L. Thyle´n, A. Talneau, and S. Anand, "Negative refraction at infrared wavelengths in a two-dimensional photonic crystal," Phys. Rev. Lett. **93**, 073902-1-4 (2004).
18. B. Momeni and A. Adibi, "An approximate effective index model for efficient analysis and control of beam propagation effects in photonic crystals," J. Lightwave Technol. **23**, 1522-1532 (2005).
19. Z. Ruan and S. He, "Open cavity formed by a photonic crystal with negative effective index of refraction," Optics Lett. **30**, 2308-2310 (2005).
20. C. Luo, S. G. Johnson, J. D. Joannopoulos, and J. B. Pendry, "Subwavelength imaging in photonic crystals," Phys. Rev. B **68**, 45115-1-15 (2003).
21. E. Cubukcu, K. Aydin, E. Ozbay, S. Foteinopolou, and C. M. Soukoulis, "Subwavelength resolution in a two-dimensional photonic-crystal-based superlens," Phys. Rev. Lett. **91**, 207401-1-4 (2003).
22. R. D. Meade, A. M. Rappe, K. D. Bromme, J. D. Joannopoulos, and O. L. Alerhand, "Accurate theoretical analysis of photonic band-gap materials," Phys. Rev. B **48**, 8434-8437 (1993).
23. B. Momeni and A. Adibi, "Systematic design of superprism-based photonic crystal demultiplexers," J. Select. Areas Commun. **23**, 1355-1364 (2005).
24. A. S. Jugessur, "Integration of a 2-D photonic crystal superprism with 1-D photonic crystal microcavity filters for high channel selectivity," TuB5 in LEOS 2005, Sydney, Australia (2005).

## 1. Introduction

Interest toward compact optical wavelength demultiplexing (WD) devices has been constantly increasing in recent years due to their potential as building blocks for spectral analysis in "lab-on-a-chip" biosensing applications and integrated optical circuits for optical information processing and communications. These WD devices are used to separate several optical channels at different wavelengths with key features being compactness (small device size), high spectral resolution (separation of channels with small wavelength difference between adjacent channels), and low cross-talk (i.e., presence of unwanted channels at the location of the desired channel). Despite the high demand for such WD devices and extensive research for their implementation, compact WD devices with required properties for practical applications have not been realized yet. A main reason has been the lack of an appropriate optical material with high dispersive properties to allow for the formation of compact structures on a chip. Recently, photonic crystals (PCs) [1-3], i.e., structures with periodic variations of refractive index (see Fig. 1(a)), have been developed as a promising material system to overcome this shortcoming.

The demonstration of the superprism effect in PCs has been a major step towards realization of PC-based demultiplexers [4-6]. The superprism effect, caused by the dispersive properties of PCs, with an appropriately designed geometry, allows for separation of multiple wavelength channels with orders of magnitude improvement in the separation angles as compared to other on-chip techniques. Since its initial demonstration, extensive research has been focused on optimizing the superprism effect for forming practical on-chip PC-based WD devices, and some proof-of-concept experiments have been reported [7,8]. However, careful evaluations have shown limited wavelength resolution for these devices [9], and dramatic increase in the size of the structures (proportional to the fourth power of the number of channels [10]), which restrict the realistic application of these demultiplexers. A main drawback in the conventional realization of the PC-based WD is the diffraction of the separated wavelength channels. The spatial broadening of these beams inside the PC calls for a large size (i.e., large propagation length) to achieve separation with reasonable cross-talk. Another (less critical) problem in conventional PC demultiplexers is the propagation of stray and unwanted light that propagate along with the separated channels resulting in added noise, especially in sensing applications.

Some improvements on the basic superprism configuration have been proposed [11-13], but the feasibility of integration remains the major challenge for the proposed structures. The

#67663 - $15.00 USD Received 3 February 2006; revised 9 March 2006; accepted 14 March 2006
(C) 2006 OSA

best experimental results for superprism-based demultiplexers reported to date show an isolation of 10 dB for only two channels 50 nm apart in wavelength using a 1250 $\mu m^2$ structure [8]. Another report demonstrates channel wavelength spacing of 20 nm but with less than 2 dB isolation in a 6300 $\mu m^2$ structure and for only two channels as well [7]. In this paper, we demonstrate a compact photonic crystal WD device with at least one order of magnitude performance improvement over the best structures reported to date. We show that the main problems of the conventional PC-based WD devices can be overcome by combining the superprism effect with two other main properties of PCs, i.e., negative diffraction and negative refraction (both studied extensively in separate contexts). Through detailed optimization of the PC structures we found PCs that can simultaneously demonstrate all these effects efficiently. The idea of diffraction compensation for efficient superprism devices has been proposed and investigated before [14-16], but no experimental demonstration has been reported to date. The WD device presented in this paper is, to the best of our knowledge, the first experimental demonstration of a PC-based wavelength demultiplexer with compact size and acceptable cross-talk.

## 2. Principle of operation

The basic ideas of the three effects that are combined in our design are shown in Fig. 1. Figure 1(a) shows a typical planar PC fabricated by etching a two-dimensional (2D) array of air holes in Si. Figure 1(b) shows the superprism effect, in which the PC separates wavelength channels by directing them into different angles. Figure 1(c) shows the application of the negative diffraction property of PCs for diffraction compensation. Propagation of an optical beam in a PC with negative diffraction index compensates for the diffraction caused by propagation through a normal (i.e., positive diffraction index) material. This property has been used for imaging based on diffraction compensation [17,18], and it has been recently proposed to realize an open cavity geometry [19]. Another property of PCs (investigated in a different context) is the negative refraction at the PC interface (as shown in Fig. 1(d)). This effect has also been studied for superlensing and imaging beyond the diffraction limit [20-21]. As Fig. 1(d) shows, the desired signal is refracted away from the direction of the incident signal (causing the separation of the desired signal from stray signals).

The key contribution of the present paper is designing PC structures that simultaneously demonstrate these three effects to optimize the wavelength demultiplexing performance. Such PCs can be used to separate wavelength channels, focus the separated channels down to a small size while propagating through the PC, and at the same time divert the separated channel from the stray and unwanted signals. Our proposed structure is an example of dispersion engineering in PCs. In our approach, we start with the band structure of the PC calculated using the plane-wave expansion technique [22] and specify regions with different dispersive properties. The band structure of a planar square lattice PC in the form of constant frequency contours in the two-dimensional wavevector plane (i.e., $k_x$-$k_y$ plane) is shown in Fig. 2. A three-dimensional supercell plane wave expansion method is used to find these band structures. Different regions with desired features of the PC dispersion (i.e., superprism, negative refraction, and negative diffraction) are marked by different colors in Fig. 2. In general, there is no guarantee for simultaneous presence of these three properties. However, by careful optimization of the geometry of the PC (i.e., lattice type, lattice constant, size of the holes, etc.), we found PC structures with this important feature.

An enabling tool for efficient analysis and optimization of PC dispersion is the PC effective index model that we have recently developed [18,14]. Using this model, different orders of diffraction for propagation in a PC structure are represented by different orders of the local derivatives of the constant frequency contours (i.e., $d^n k_l / dk_t^n$, with $k_l$ and $k_t$ being the longitudinal and transverse wavevectors, respectively, defined with respect to the direction of propagation of the beam) in the band structure. For example, beam broadening (ordinary diffraction) is caused by the second order diffraction and thus positive or negative diffraction can be implemented by designing the PC with positive or negative $d^2 k_l / dk_t^2$. This is the main technique we used to design PC demultiplexers with appropriate diffraction compensation.

#67663 - $15.00 USD Received 3 February 2006; revised 9 March 2006; accepted 14 March 2006
(C) 2006 OSA

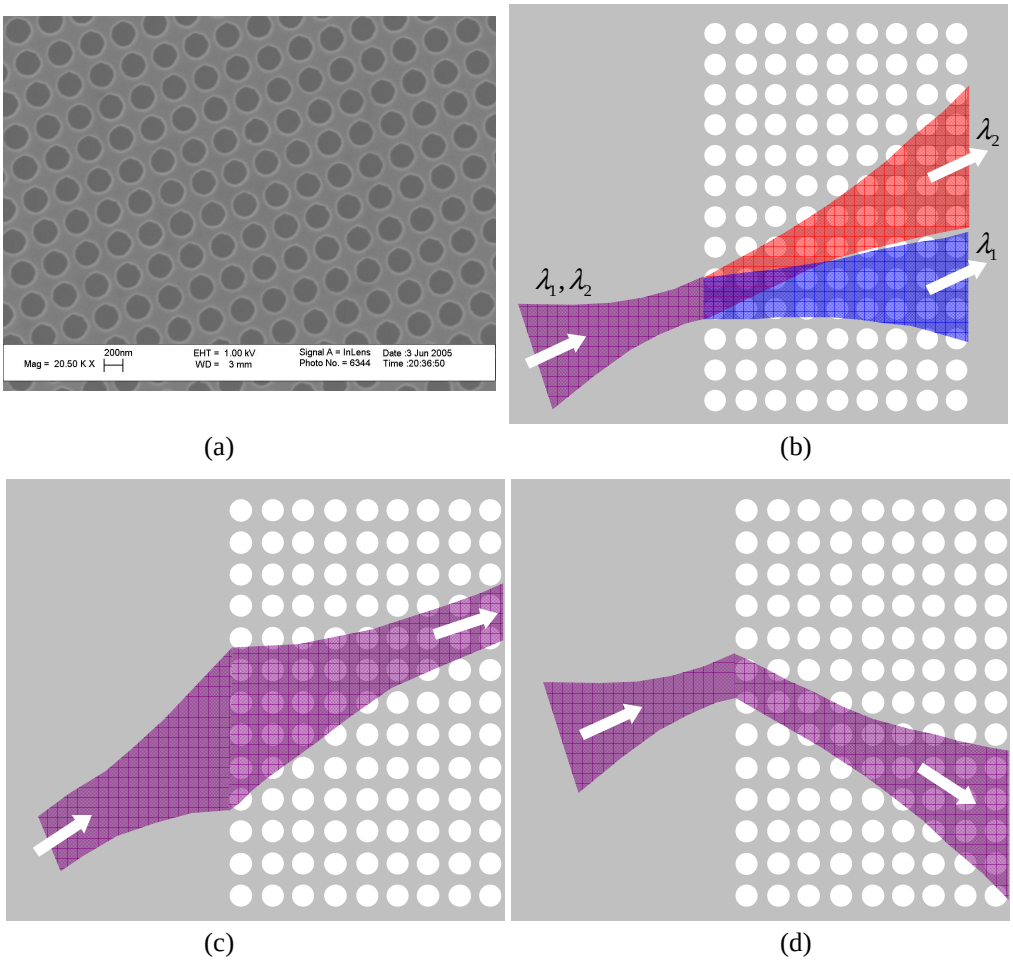


Fig. 1. (a) SEM image of a square lattice photonic crystal fabricated in SOI. (b) Schematic plot of superprism demultiplexing in conventional configuration. (c) Schematic plot of diffraction compensation (PC is designed in negative diffraction regime). (d) Schematic plot of negative refraction at the interface of PC.

The principle of operation of our proposed PC WD device is shown in Fig. 3(a), which depicts an image of the fabricated PC-based WD in a Silicon-on-Insulator (SOI) substrate. Before entering into the PC region, the incident optical beam (with multiple channels) propagates (and diffracts) in the unpatterned Si. This propagation results in a second-order spectral phase term in the spatial spectrum of the beams (and therefore, broadening of the incident beam), which we will refer to as preconditioning. As the beams propagate through the PC, they experience three basic effects: superprism effect, negative diffraction, and negative refraction. Beams of different wavelengths propagate in different directions inside the PC (superprism effect), and at the same time, the second-order spectral phase term is decreased (since the PC second-order diffraction is opposite to that of unpatterned Si) until it completely vanishes at the output (diffraction compensation), retrieving a small spot size for the beams at the output ports. Using this scheme, the spatial separation needed inside the PC region can be of the order of the minimum spot size of the incident beams, which is much smaller than its broadened version obtained in a conventional superprism demultiplexer [10]. Analytical estimates based on the effective index model show that using this scheme, the required area of the structure to achieve efficient demultiplexing scales as $N^{2.5}$ ($N$ being the

#67663 - $15.00 USD Received 3 February 2006; revised 9 March 2006; accepted 14 March 2006
(C) 2006 OSA

number of wavelength channels of the demultiplexer) [14], compared to $N^4$ dependence in the conventional PC demultiplexers [23]. Finally, the negative refraction of the separated channels results in their separation from undesired light (noise, scattering, unwanted polarization, and out-of-range wavelengths) in the incident beam, thus reducing the overall noise level.

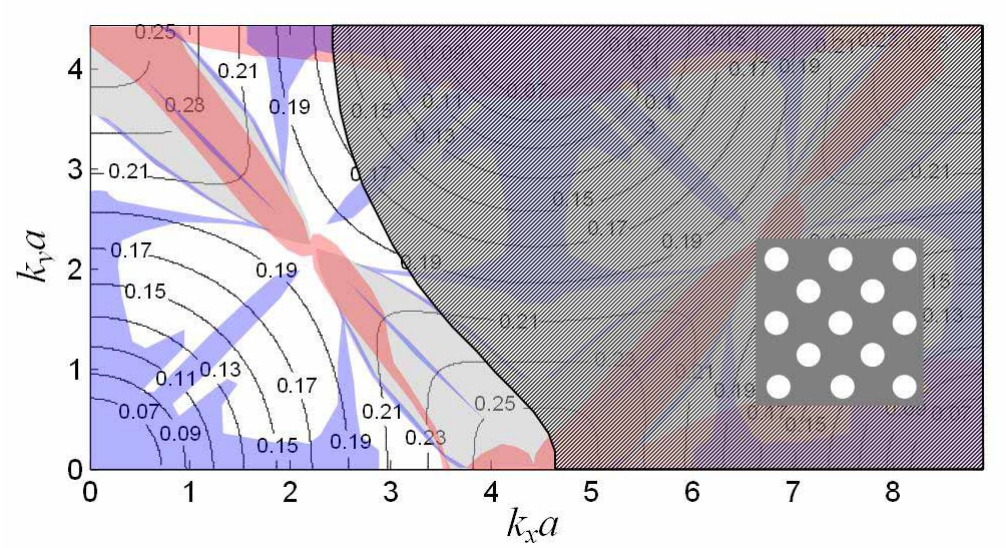


(a)

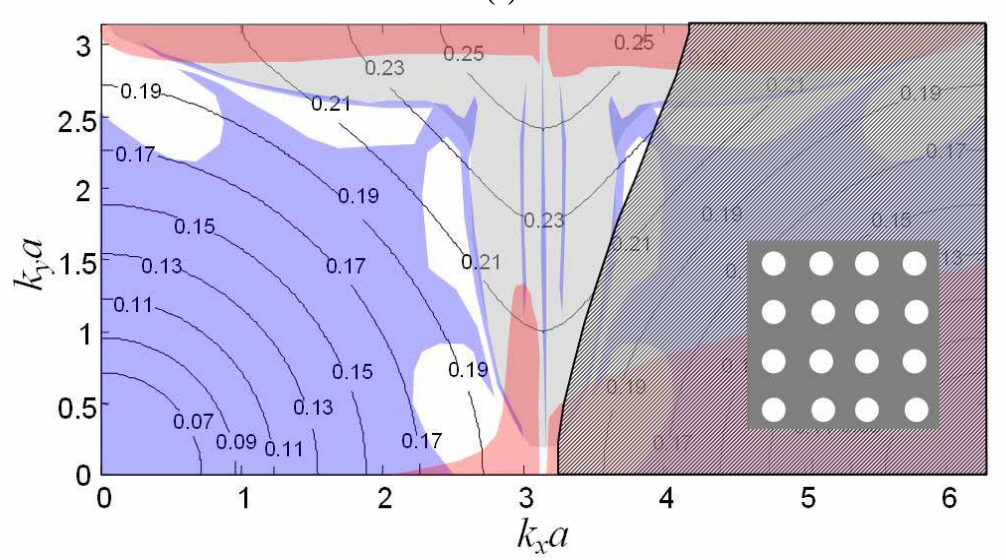


(b)

Fig. 2. Calculated contours of constant frequency of the first TE-like modes in a planar square lattice photonic crystal ($r/a$ = 0.25 on an SOI wafer) with one principal lattice direction (a) at 45-degrees with respect to the interface, and (b) parallel to the interface of the photonic crystal with incident region. Regions of band structure with different dispersion properties are marked as gray for negative diffraction ($d^2k_t/dk_i^2 < 0$) [18]; red for strong superprism effect ($\partial\theta_g/\partial\alpha >$ 50, where $\theta_g$ is the angle of group velocity and $\alpha$ is the angle of incidence [10]); blue for low third-order diffraction (small ($\partial n_e/\partial\alpha$, where $n_e$ is the effective diffraction index [18]), and hatched for regions that cannot be excited from the input slab waveguide. The loci where these three colored regions overlap have strong superprism effect, negative diffraction, and negative refraction, simultaneously.

#67663 - $15.00 USD Received 3 February 2006; revised 9 March 2006; accepted 14 March 2006
(C) 2006 OSA

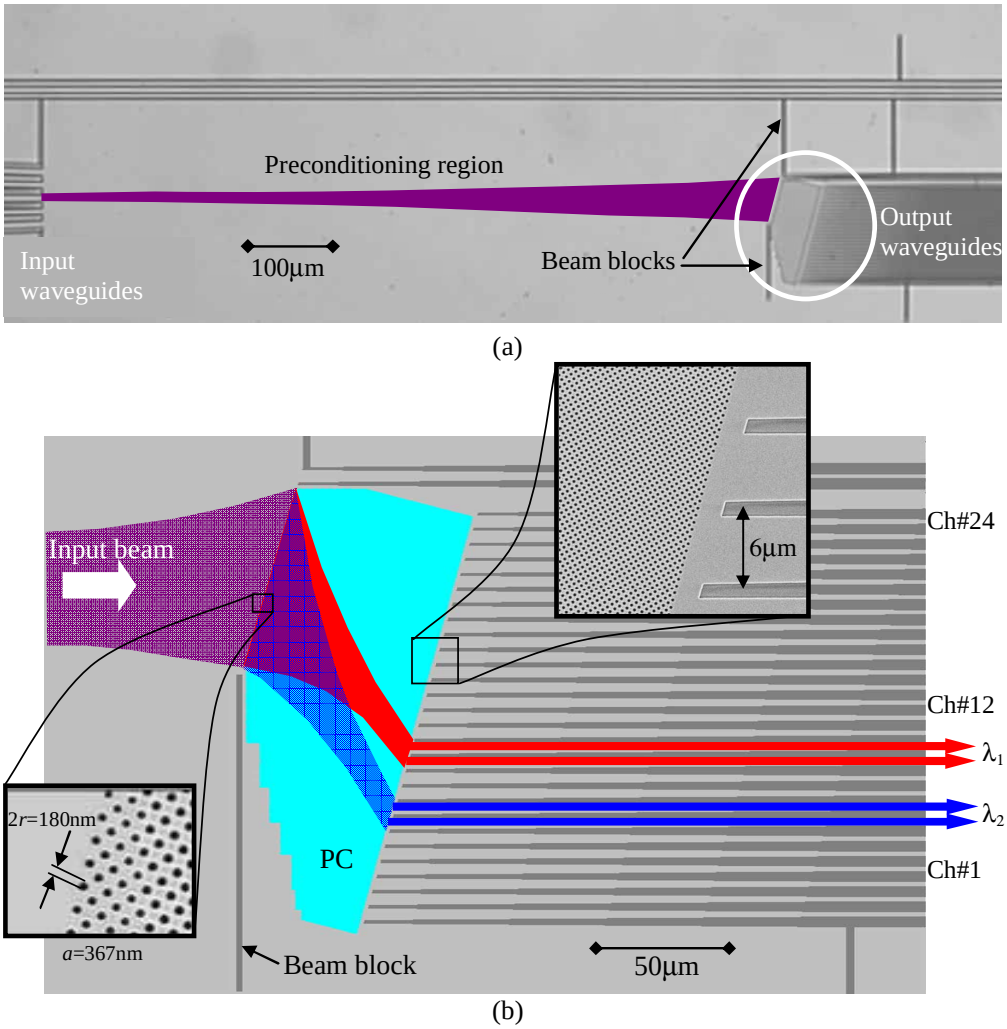


Fig. 3. (a) Top view image of the preconditioned demultiplexing device is shown. (b) Photonic crystal region and output waveguides (highlighted region in (a) are schematically depicted. Insets show SEM images of a portion of the PC structure at the input interface (bottom), and at the entrance to output waveguides (top) to show the details of the periodic structure. Beam propagation and spatial separation process are schematically shown for two channels (red and blue). The photonic crystal structure is a square lattice which is 45°-rotated with respect to the input interface of the PC.

A key condition for the optimization of the proposed WDs is the reduction of the role of the higher-order diffraction effects. Since the second-order dispersion is fully compensated in our proposed structure, the third-order diffraction (related to $d^3k_i/dk_i^3$) becomes the dominant factor in broadening the beams. To minimize the output beam size, we need to engineer the dispersion of the PC to have minimum third-order diffraction in addition to all three properties discussed before. Thus, the optimization criteria for the proposed preconditioned WD are different from those for the conventional superprism-based demultiplexers. We modified a recently proposed systematic technique for the optimization of the conventional superprism-based PC demultiplexer [23] by incorporating the condition for $d^3k_i/dk_i^3$ in the preconditioned superprism WD devices [14]. Using this new criterion, we found that a rotated square lattice structure is in general the most suitable for preconditioned WD devices. The optimum

#67663 - $15.00 USD Received 3 February 2006; revised 9 March 2006; accepted 14 March 2006
(C) 2006 OSA

operating point in this case lies on one of the symmetry directions of the lattice band structure where the third order diffraction vanishes due to the inherent symmetry of the structure. Another advantage of our proposed structure over previously reported structures is working in the first (TE-like) band of the PC (compared to previous reports that use PCs in their second band). It is known that coupling to leaky waves is considerably less if the operation is limited to the first band. Thus, we expect our proposed structure to have lower propagation loss compared to conventional PC-based WD devices assuming similar fabrication accuracy.

### 3. Characterization results

The optimal structure found by dispersion engineering of the PC according to the guidelines mentioned in the previous section was fabricated on a SOI wafer with 3 μm of $SiO_2$ sandwiched between a thick Si substrate and a 220 nm layer of Si (on top) covered by 50 nm of $SiO_2$ that is used as a hard-mask during the fabrication process. The 2D PC pattern is lithographically written on the top $SiO_2$ layer using a JEOL JBX-9300FS 100kV electron beam lithography system and then etched using a Plasma-Therm inductively coupled plasma (ICP) system with an optimal chlorine-based etch chemistry. Figure 3 shows the schematic view of the fabricated structure. Light is end-coupled into the structure through one of a series of 10.6 μm wide input waveguides each exciting the PC structure at a unique incident angle in the range of 13 to 17 degrees. The PC region (found through optimization) has a 45°-rotated square lattice geometry with a lattice constant of 367nm and with holes of 180nm in diameter, as shown in the inset of Fig. 3. The propagation through the 1100 μm long unpatterned Si region (schematically shown in Fig. 3) preconditions the beam with positive second order phase. Beam blocks are used at the entrance of the PC region to limit the spatial-spectral content of the input beam (i.e., to spatially filter out some of the higher-order beams that are excited by higher order modes of the multimode input waveguide) and also to prevent stray incident light from reaching the output end. The output light of the PC region is coupled into an array of 5 μm wide waveguides (1 μm distance between neighboring waveguides) to obtain better spatial resolution (note that the size of beam for each wavelength channel is around 11 μm at the output). The spatial extent of light in each wavelength channel in the PC demultiplexer output corresponds to two output waveguides. Each output waveguide is tapered down to 2 μm at the output end of the devices. Two of the wavelength channels are schematically shown on Fig. 3 as red and blue curves.

In our measurement setup, shown in Fig. 4, a tunable laser (81680A from Agilent Technologies, covering 1460 nm to 1580 nm wavelength range) is coupled to a graded refractive index (GRIN) fiber lens and the collimated beam is directed through a broadband polarizer to assure the right polarization of input beam. A 40x objective lens is used to end-couple the light into one of the input waveguides of the devices. An infrared (IR) camera connected to a long working distance microscope is used to monitor the coupling to the input waveguide from the top. The output edge of the device is imaged using a 20x objective lens on another IR camera. Half of the output light intensity is directed to an IR detector (New Focus #2033 with 30 kHz bandwidth) by a broadband beam splitter, which is connected to a lock-in amplifier (Stanford Research Systems, SR830) with a modulation frequency of 20 kHz to enhance the signal-to-noise ratio of the measurement.

Figure 5(a) shows the image of the output waveguides at four discrete wavelengths with input in TE-like polarization (electric field parallel to the plane of periodicity). Good separation of these wavelength channels can be clearly seen in Fig. 5(a). In addition, the desired small spot from diffraction compensation effect is evident from this figure (note that the size of the input beam at the entrance to the PC region is around 60μm). Another evidence for dramatic minimization of the output spot size comes from the comparison of the focusing TE-like beams with TM-like beams for which neither the superprism effect nor the diffraction compensation occur.

#67663 - $15.00 USD Received 3 February 2006; revised 9 March 2006; accepted 14 March 2006
(C) 2006 OSA

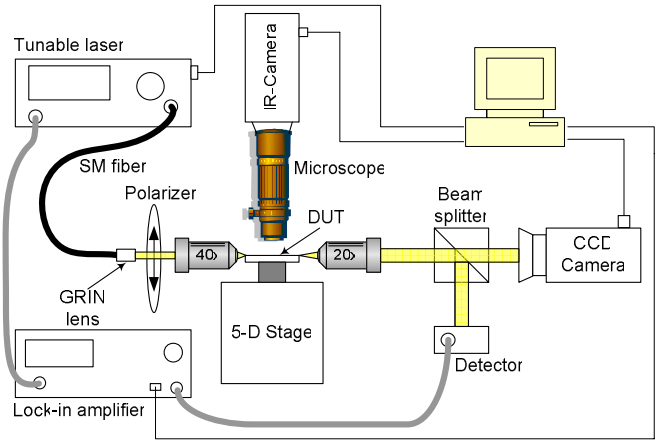


Fig. 4. Setup for characterization of preconditioned superprism-based photonic crystal demultiplexer is shown.

In Fig. 5(b), we show the measured output distributions for TM-like polarization for the same set of wavelengths used in Fig. 5(a). It can be easily seen that the overall output beam profiles of all TM-like channels are very broad, covering more than 10 output waveguides. Comparing Figs. 5(a) and (b), the effect of negative diffraction in refocusing the TE-like polarization beams at the output end is evident. Also, it can be clearly observed that by designing the device in the negative refraction regime for TE polarization, the unwanted polarization (TM) is successfully isolated from the desired signals (i.e. all TM signals in the wavelength range of operation appear in a separate set of output waveguides). In order to measure the power in each output waveguide, a pinhole in the far-field of the device output is used to select only a single waveguide and to reduce the scattered light from the background.

The normalized measured power for four of the output waveguides at 15° incident angle from the input waveguide are shown in Fig. 6(a). Four channels are separated in this device with a wavelength spacing of 8nm, and channel isolations (sum of contributions of other channels at the location of the desired one) are better than 6.5dB. This is to the best of our knowledge the first demonstration of an integrated superprism-based demultiplexing device with such channel separation in a 4500 $\mu m^2$ (i.e., 50μm×90μm) PC structure. Using the same scheme, a 64-channel demultiplexer with channel spacing of 0.5 nm can be realized in a 4 $mm^2$ PC structure.

Another advantage of the preconditioned PC demultiplexers over the conventional ones is the low sensitivity to the divergence angle of the incident beams [14]. In conventional structures, the incident beam has to be highly collimated for proper operation since the divergence angle of the beam directly determines the broadening of the beam inside the structure that in turn determines the requirement for spatial separation. In preconditioned PC demultiplexers, however, the second-order diffraction is eliminated throughout the structure, and the divergence angle of the input beam only has to be small enough to avoid excessive broadening caused by the higher-order effects (which are much weaker than the second-order effect). Analytical derivations [14] show that the required divergence angle of the preconditioned PC demultiplexers scales as $N^{-1/2}$ ($N$ is the number of demultiplexing channels), as opposed to $N^{-1}$ dependence in conventional PC demultiplexers [10]. Noting that small divergence angles require highly collimated beams that are hard to achieve in an integrated platform, this is a significant improvement from a practical point of view for realizing an integrated demultiplexer working at high resolution. Finally, our proposed device focuses all the power of each channel in its corresponding region (i.e., output waveguide) with minimal presence of the signal from other channels as shown in Fig. 3. This is a major

#67663 - $15.00 USD Received 3 February 2006; revised 9 March 2006; accepted 14 March 2006
(C) 2006 OSA

advantage of our WD device over implementations that rely on heavily reducing the throughput for improving cross-talk as done in Ref. [24].

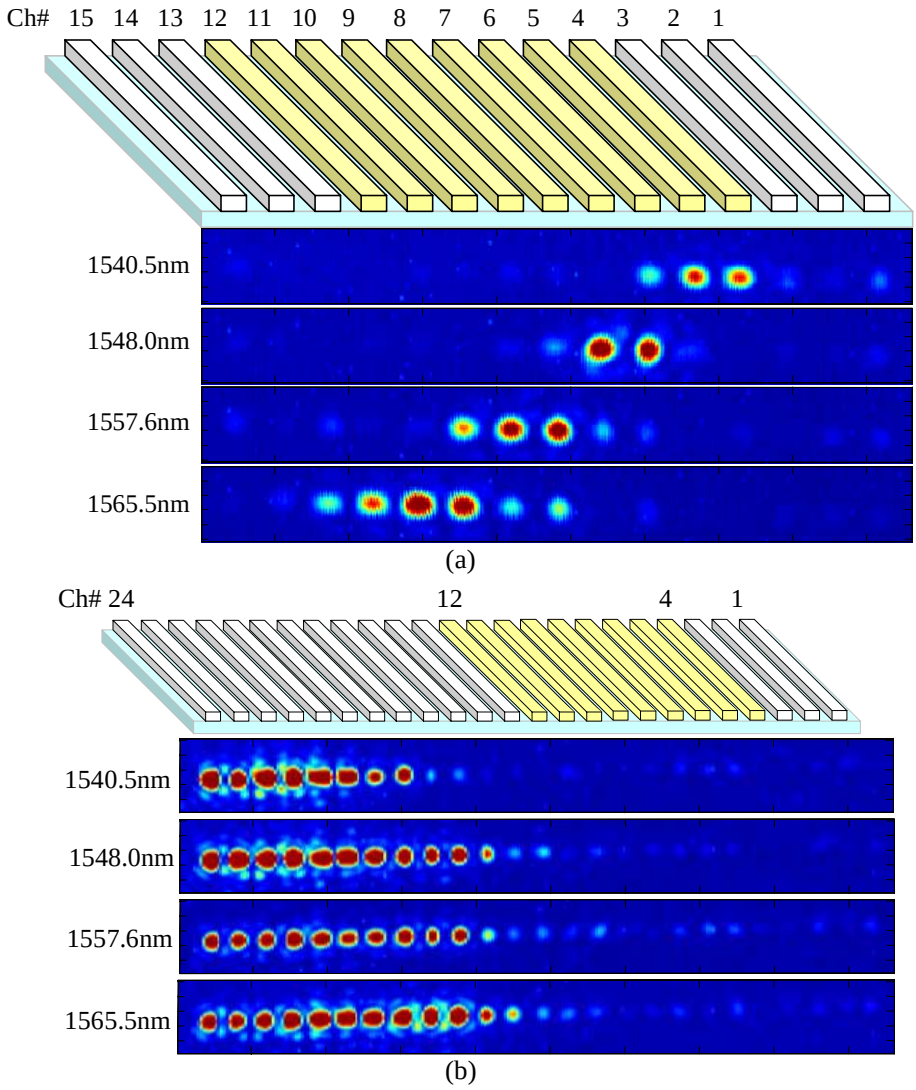


Fig. 5. (a) Output image for TE-like polarization shows power distribution in the output waveguides for four discrete wavelengths. (b) For the same wavelength as part (a), power distributions in the output waveguides for TM-like polarization are shown. It can be seen that for this polarization diffraction compensation does not occur, and output beams have extended distributions. Moreover, there is negligible interference from this polarization at the location of demultiplexing channels highlighted in this figure.

Note that in general, the power level for different channels is not uniform (1.5 dB variation over the channels is shown in Fig. 6) due to either the wavelength-dependent intrinsic loss of the PC, wavelength-dependent nonuniformity in excitation, or quality of end-face of output waveguides corresponding to different channels. Note also that for the fourth channel (at 1563 nm in Fig. 6) the focusing is not as good as the other channels. Possible reasons for the side-lobe appearing on one side of the spectrum (visible on the two channels on the right in Fig. 6(b)) are distortion in the incident beam and diffraction effects from beam

#67663 - $15.00 USD Received 3 February 2006; revised 9 March 2006; accepted 14 March 2006
(C) 2006 OSA

blocks at the entrance to the PC region, and residual third-order spatial diffraction effects (possibly caused by imperfections in fabrication that deviate the fabricated structure from the optimum operation point with low spatial dispersion effects). The total insertion loss for the sample demonstrated in this paper is estimated to be 13 dB by comparing the output power level to that of a straight ridge waveguide on the same substrate. Note that a large portion of this loss (approximately 6 dB) is due to the multimode nature of the input waveguide and can be considerably reduced by using a tapered input waveguide. We are considering further improvement in the excitation configuration as well as optimization of the geometry of the PC to enhance the performance of the device. The preconditioning region in Fig. 3 is chosen to be an unpatterned Si slab for simplicity of demonstration. In a practical device, this region will also be designed with PCs with positive index of diffraction to further reduce the size.

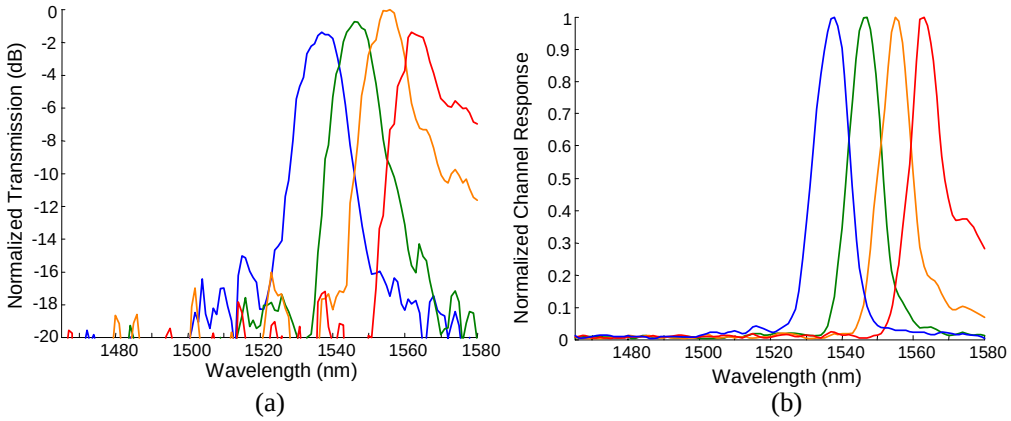


Fig. 6. (a) Measured transmitted powers of four output waveguides (channels 5, 7, 9, and 11) are plotted. (b) Channel response for the waveguides in (a) are shown. In this case, incidence is at 15 deg. (middle input waveguide is used for excitation), and input wave is in TE-like polarization.

## 4. Conclusion

We have demonstrated here a compact photonic crystal wavelength demultiplexing device by simultaneously combining three unique dispersion properties of photonic crystals (superprism effect, negative refraction, and diffraction compensation) to achieve the best experimental on-chip demultiplexing performance reported to date. Compared to the conventional implementation, the new preconditioned superprism-based photonic crystal demultiplexers are more compact and have a less-demanding requirement for the divergence angle of the incident beam. Due to much slower increase of the size of the preconditioned demultiplexer with the number of wavelength channels ($N$) compared to the conventional implementation ($N^{2.5}$ instead of $N^4$ variation), we expect the size of the preconditioned structure to be several orders of magnitude smaller than that of the conventional devices for practical wavelength resolutions and numbers of channel. Thus, this new implementation opens up many possibilities for applications including compact spectrometers (for sensing applications) and WD for communication systems.


## Acknowledgments

The authors would like to thank C. M. Reinke for useful discussions.



#67663 - $15.00 USD Received 3 February 2006; revised 9 March 2006; accepted 14 March 2006


(C) 2006 OSA